Electric Supplementary Information

Control of the Photoluminescence Properties of Single-walled Carbon Nanotubes by Alkylation and Subsequent Thermal Treatment

Yutaka Maeda, Yuya Takehana, Michio Yamada, Mitsuaki Suzuki, Tatsuya Murakami
Department of Chemistry, Tokyo Gakugei University, Tokyo 184-8501, Japan
Institute for Integrated Cell-Material Sciences (WPI-iCeMS), Kyoto University, Kyoto 606-8501, Japan

Experimental section

Experimental Section

Methods

(6,5)-enriched SWNTs (SG 65i) was purchased from Sigma-Aldrich. Butyllithium and butyl bromide were purchased as reagent grade from commercial suppliers. Optical absorption spectra were recorded through a Pyrex cell with 10 mm path length using a spectrophotometer (V-670; Jasco Corp.). Raman spectra were measured using a spectrophotometer (LabRAM HR-800; Horiba Ltd.) under excitation at 514.5 or 633 nm. The Raman spectra are normalized to the G-band. Photoluminescence spectra were measured using the spectrophotometer equipped with a 450 W lamp and a Symphony-II CCD detector (Nanolog; Horiba Ltd.). The excitation wavelength was varied from 500 to 1000 nm in 1 nm steps, whereas the emission wavelength was varied from 900 to 1600 nm in 1 nm steps. The excitation spectral and the emission slit widths were 10 nm, respectively. The PL intensity was corrected to allow a comparison by the lamp intensity at each wavelength and by the data correction time of the each sample. TGA was performed at a heating rate of 10 °C/min and a nitrogen flow rate of 50 ml/min (TG-50A; Shimadzu Corp.). Ultrasound irradiation was performed using a bath sonicator (B2510J-MT ultrasonic cleaner; Branson). Centrifugation was performed using a high speed refrigerated centrifuge with a P70AT2 angle rotor (CP80β; Hitachi Koki Co., Ltd.). Scanning electron microscope (SEM) observation was conducted using a field emission electron microscope (1.5 kV accelerating voltage, 10 mA beam current, SU8020; Hitachi Ltd.).

Typical procedure of two-step reductive alkylation:

In a 200 ml heat-dried three-necked round-bottom flask, 5.0 mg of SWNTs and 50 ml of anhydrous benzene were placed and then sonicated for 30 min under argon at 5 ˚C. To this dispersion was added 2.13 mL of butyllithium (**1**, 3.3 mmol) in pentane. After the resulting suspension of an alkylated SWNTs anion (Bu-SWNTs-Li^+) was stirred for 30 min, it was sonicated for 30 min. Then butyl bromide (**2**, 6.4 mmol) was added to the mixture. The mixture was sonicated for 1 h and then quenched by addition of 15 ml of dry ethanol. The reaction mixture was washed with water and diluted in 1.0 M HCl aq. and then was washed with $NaHCO_3$ aq. until the pH value remained neutral. The suspended black solid was collected by filtration using a membrane filter (PTFE, 1.0 mm) and washed with tetrahydrofuran, methanol, and dichloromethane using the dispersion-filtration process. The solid was dried under vacuum at 50 °C.

Thermal treatment of dialkylated SWNTs

Thermal treatment of Bu-SWNTs-Bu was performed at a heating rate of 10 °C/min and a nitrogen flow rate of 50 ml/min using a thermogravimetric analyzer (TG-50A; Shimadzu Corp.). After attainment of the preset temperature, the heating furnace was cooled using a cooling blower (BLW-50 cooling blower; Shimadzu Corp.).

Preparation of SWNTs dispersion using SDBS in D_2O:

SWNTs or functionalized SWNTs (Bu-SWNTs-Bu) (0.1 mg) were added to 6 ml of D_2O containing 1 wt% sodium dodecyl benzene sulfonate (SDBS) and sonicated for 1.5 h in a bath-type sonicator. This suspension was then centrifuged for 1 h at 140000 g and the supernatant solution was used for absorption and photoluminescence measurement. For adjustment of absorption intensity around 775 nm, adequate dose of D_2O solution containing SDBS was added to the dispersion depending on the absorption spectra. After sonication, the resulted suspension was centrifuged for 1 h at 140000 g.

The PL spectra of various concentrated dispersions of SWNTs and *n*Bu-SWNTs-*n*Bu were measured (see Supplementary Information, Figure S14). The absorption intensities of SWNTs and *n*Bu-SWNTs-*n*Bu for PL measurements are listed (Supplementary Information, Table S1).

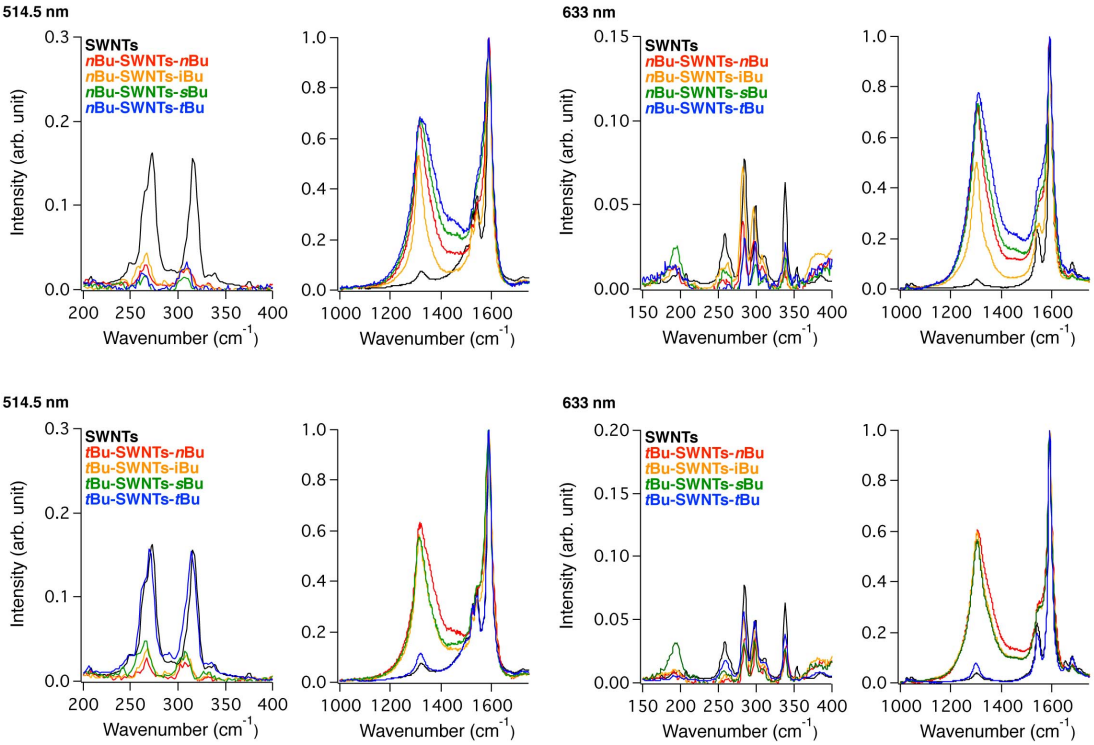

Figure S1. Raman spectra of SWNTs and Bu-SWNTs-Bu normalized to G-band intensity.

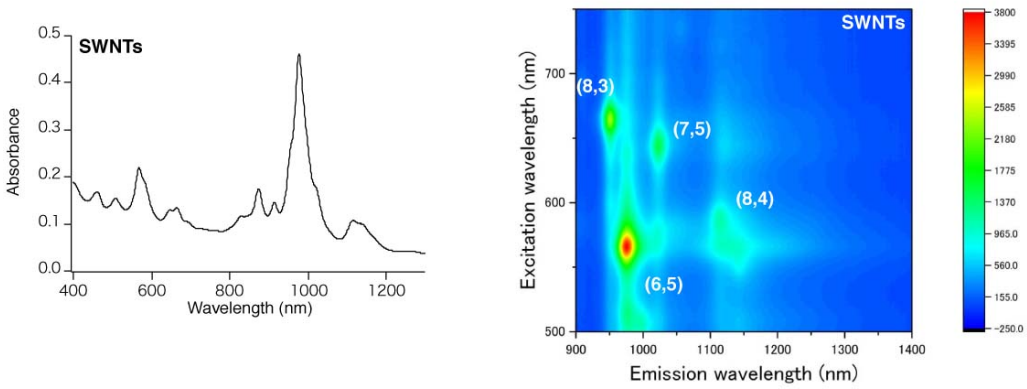

Figure S2. Absorption spectrum and contour plots of fluorescence intensity versus excitation and emission wavelength of SWNTs.

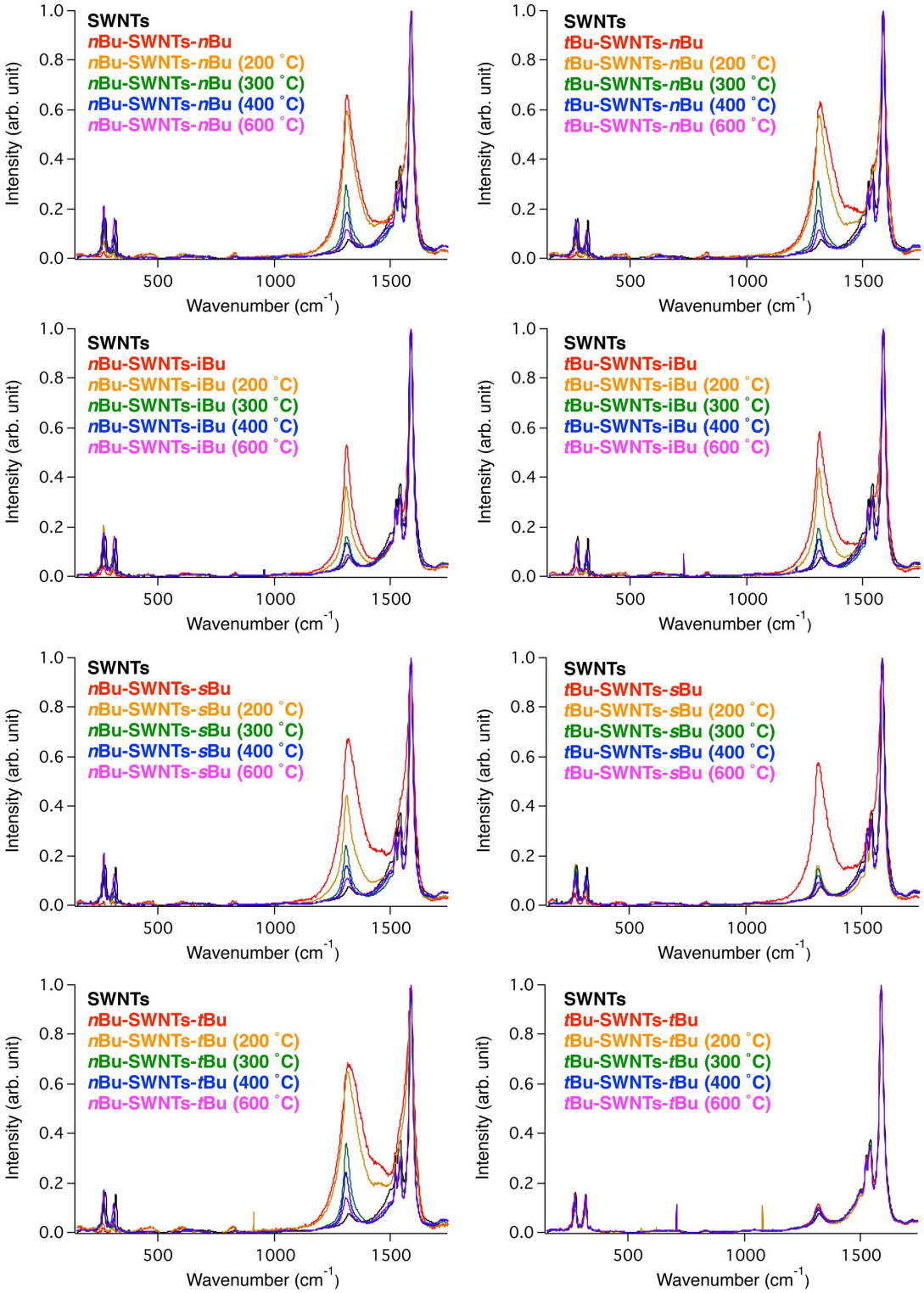

Figure S3. Raman spectra of SWNTs and Bu-SWNTs-Bu after thermal treatment normalized to G-band intensity excited at 514.5 nm.

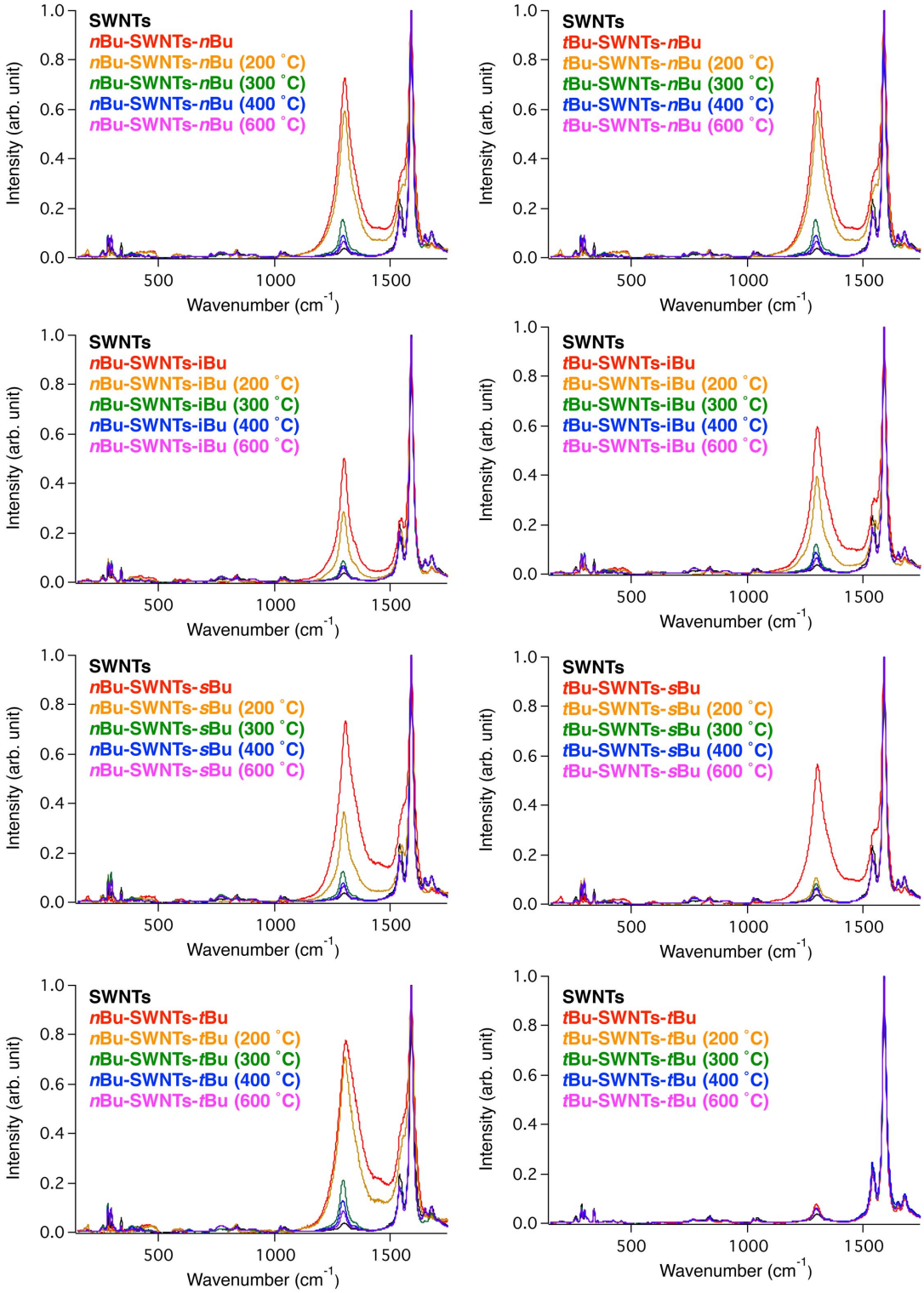

Figure S4. Raman spectra of SWNTs and Bu-SWNTs-Bu after thermal treatment normalized to G-band intensity excited at 633 nm.

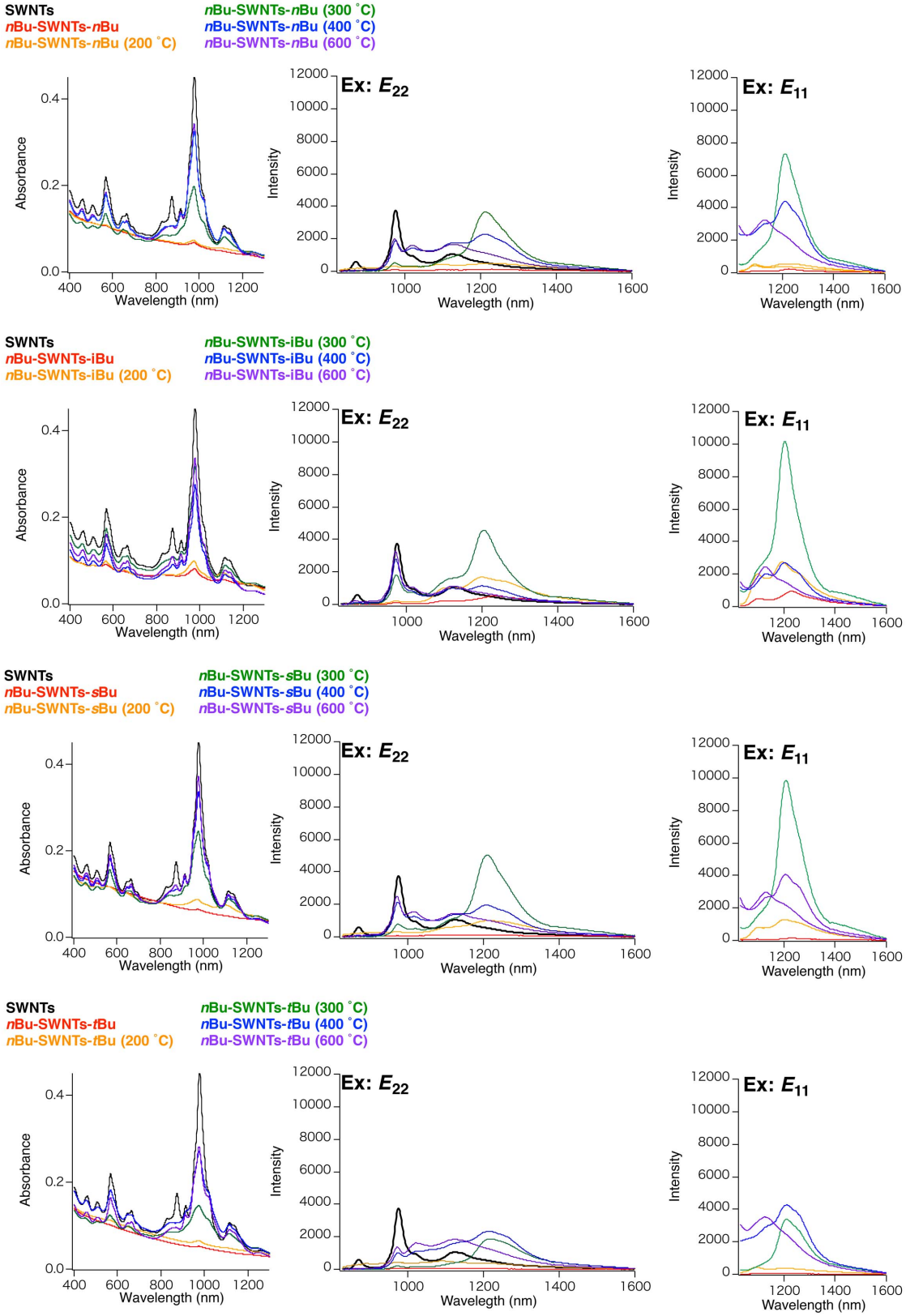

Figure S5. Absorption and photoluminescence spectra of SWNTs and *n*Bu-SWNTs-Bu after thermal treatment.

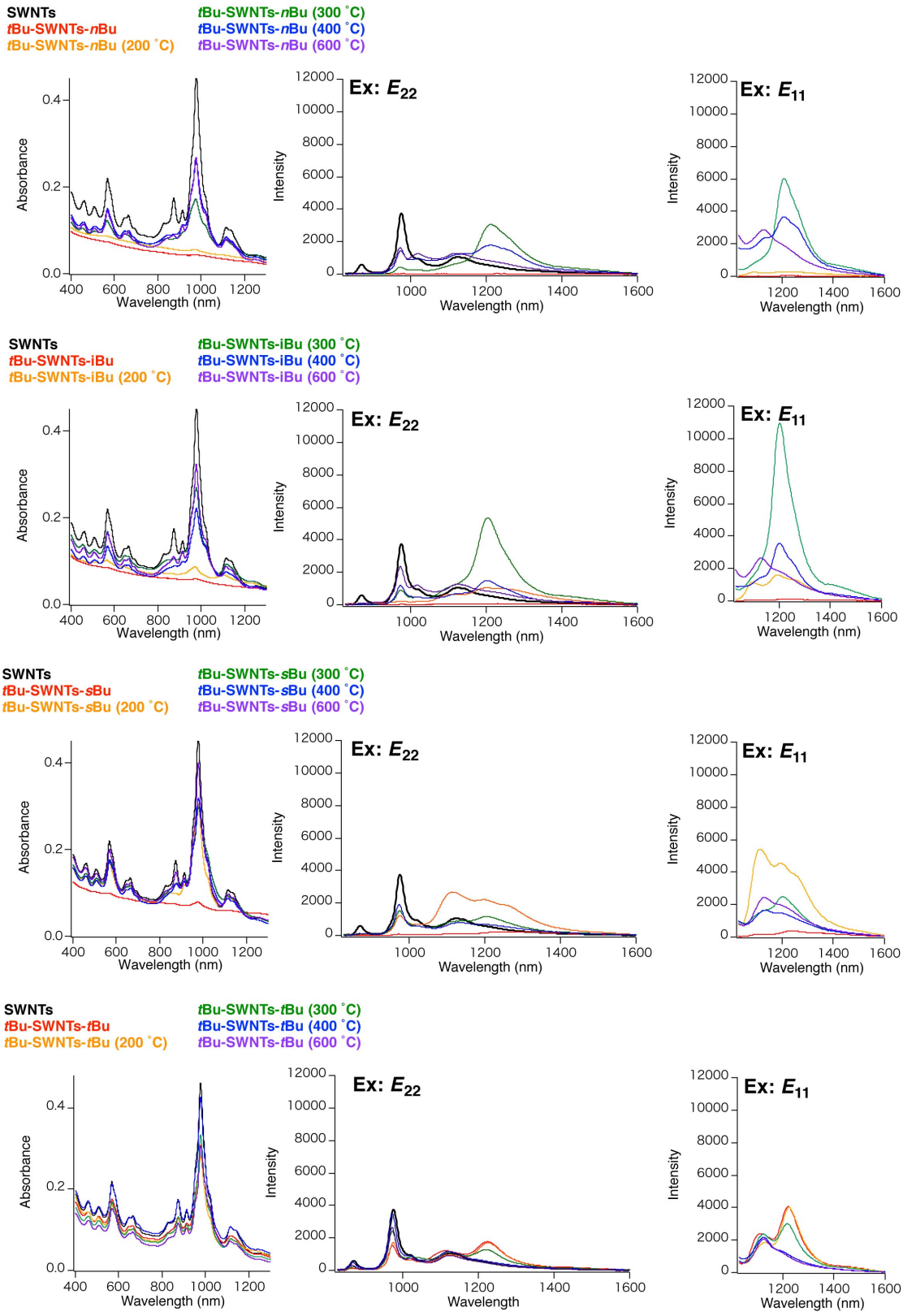

Figure S6. Absorption and photoluminescence spectra of SWNTs and *t*Bu-SWNTs-Bu after thermal treatment.

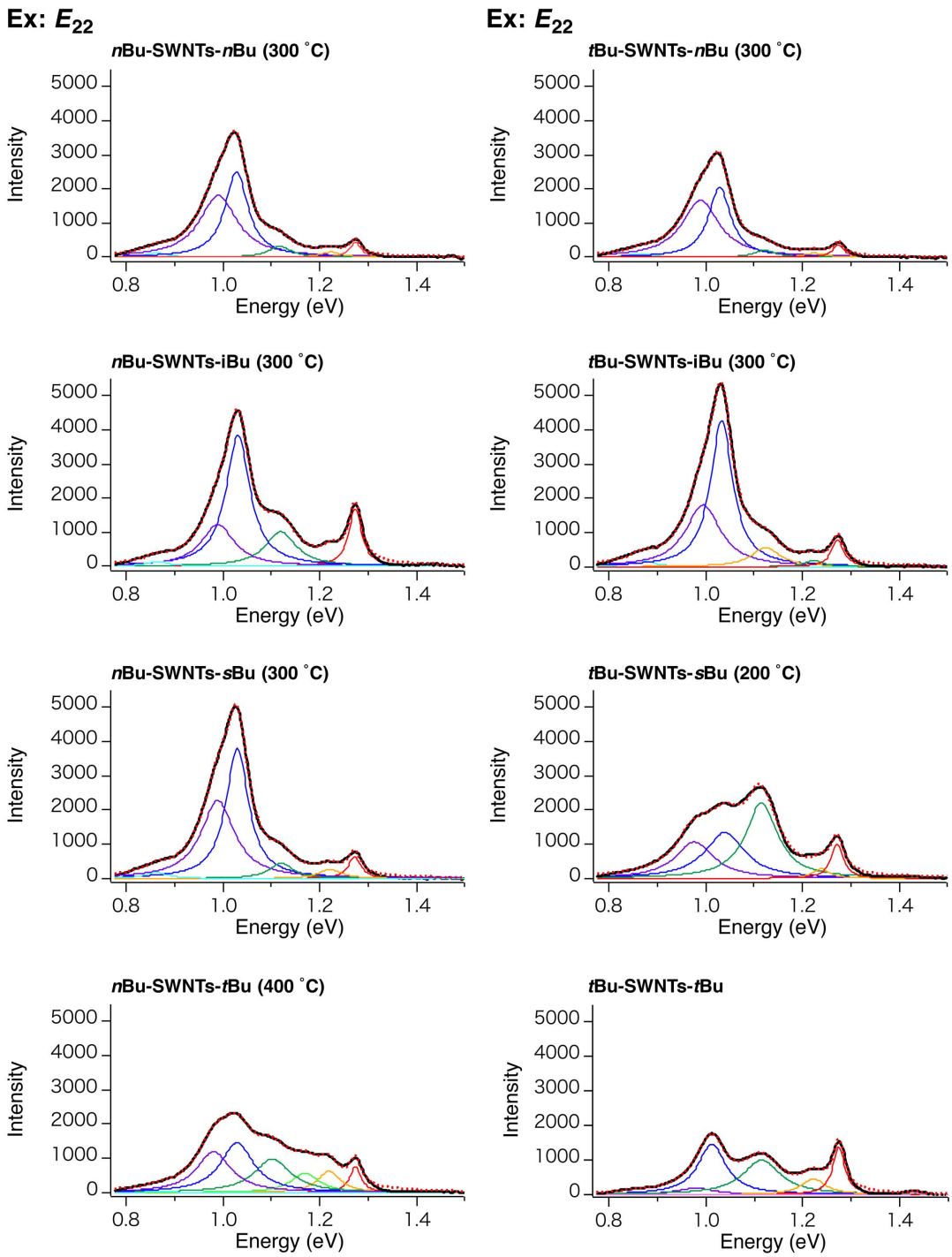

Figure S7. Photoluminescence spectra of Bu-SWNTs-Bu after thermal treatment with excitation wavelength of E_{22}. Black line: PL spectra. Colored line: Lorentzian curve fitting. Dashed line: Sum of curve fitting data.

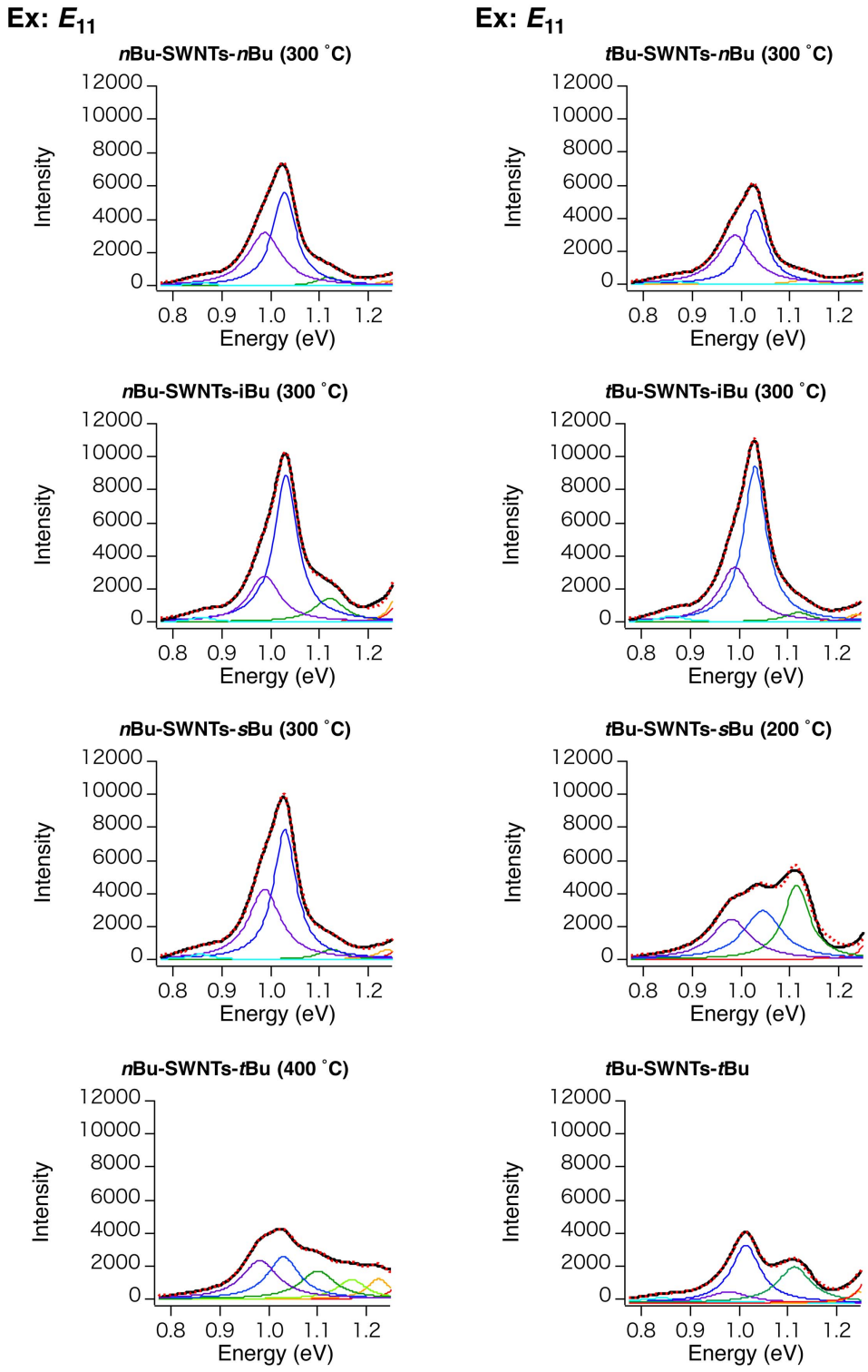

Figure S8. Photoluminescence spectra of Bu-SWNTs-Bu after thermal treatment with excitation wavelength of E_{11}. Black line: PL spectra. Colored line: Lorentzian curve fitting. Dashed line: Sum of curve fitting data.

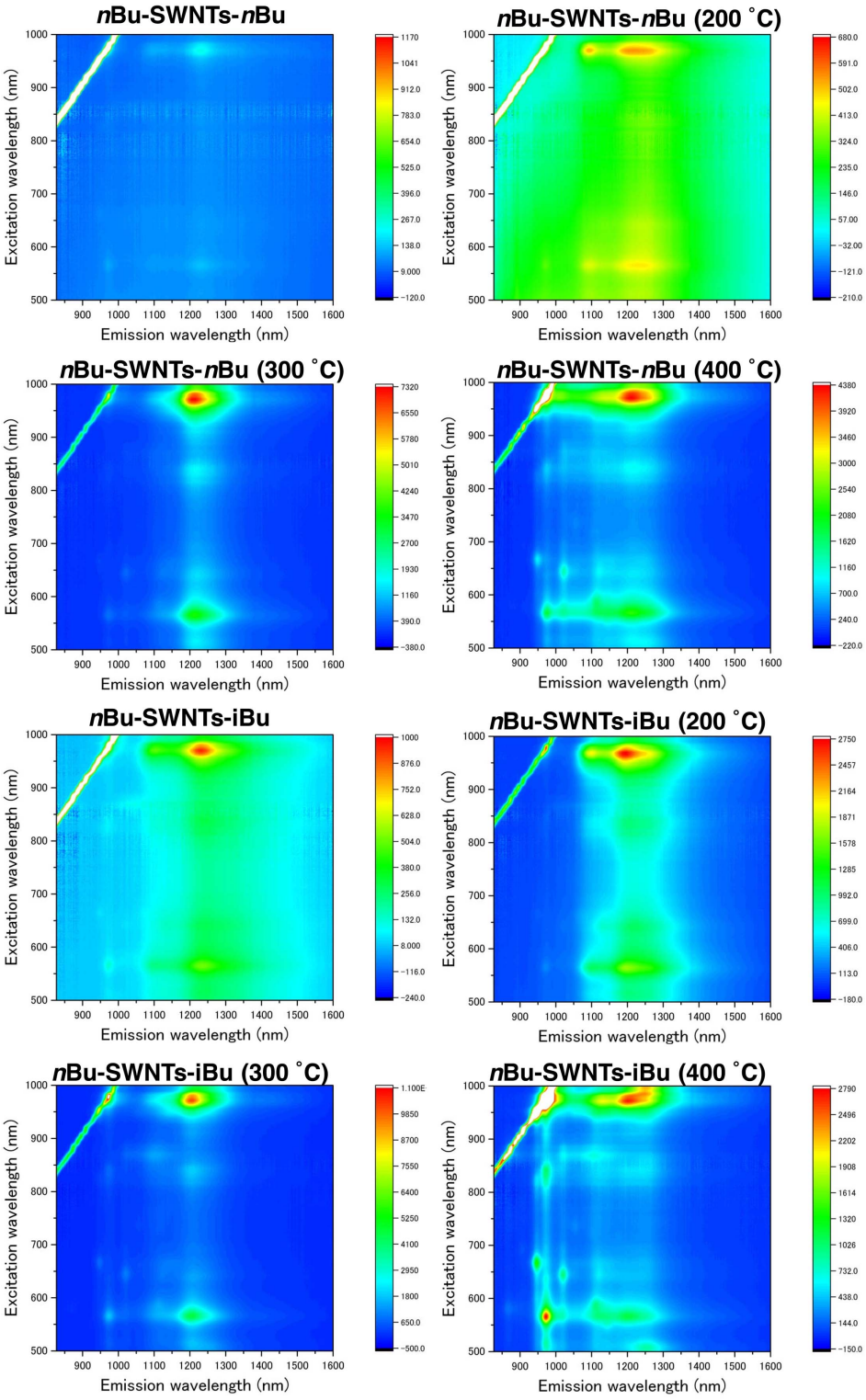

Figure S9. Contour plots of fluorescence intensity versus excitation and emission wavelength of SWNTs and *n*Bu-SWNTs-Bu before and after thermal treatment. The SWNTs were dispersed in D_2O containing SDBS.

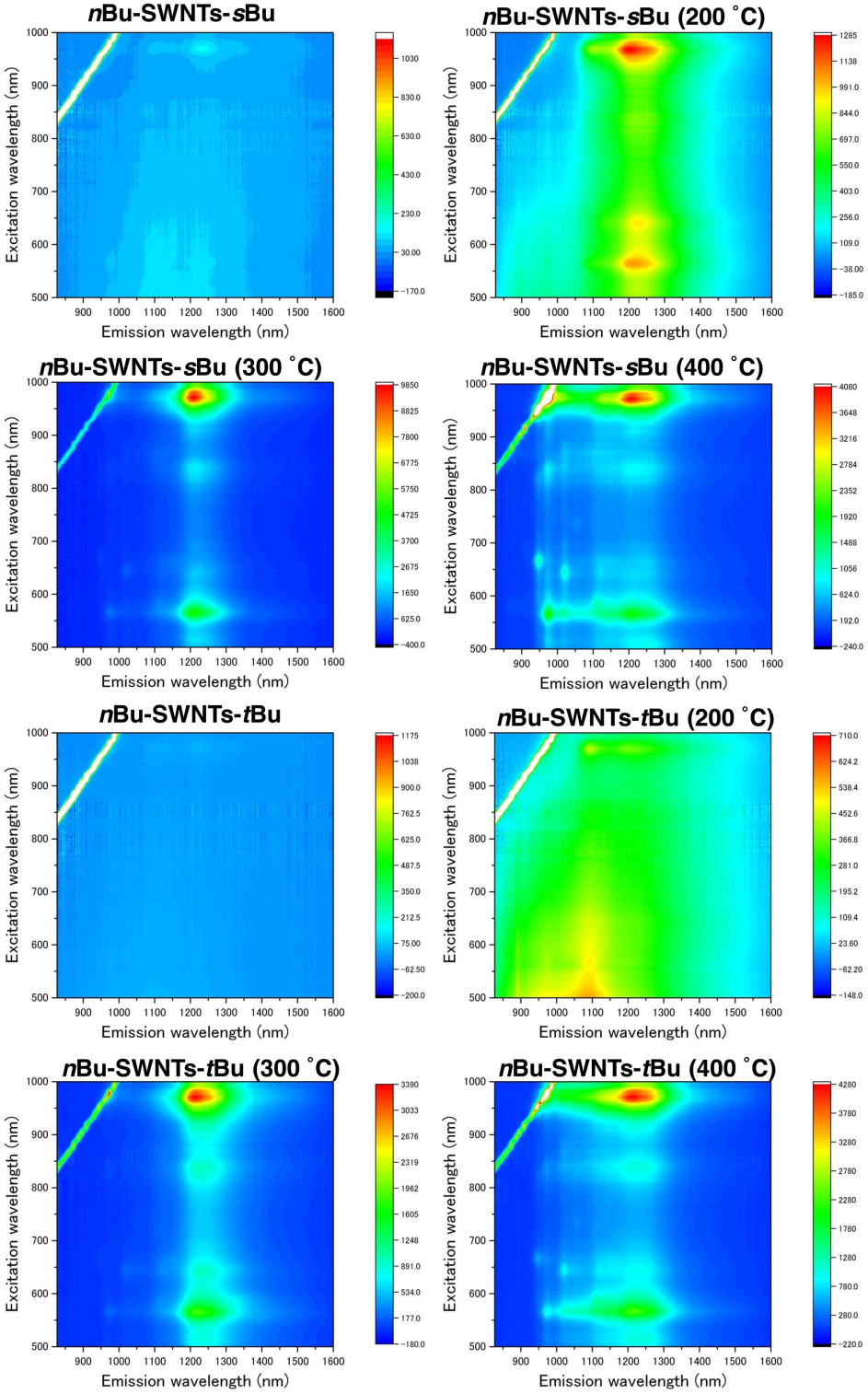

Figure S10. Contour plots of fluorescence intensity versus excitation and emission wavelength of SWNTs and *n*Bu-SWNTs-Bu before and after thermal treatment. The SWNTs were dispersed in D_2O containing SDBS.

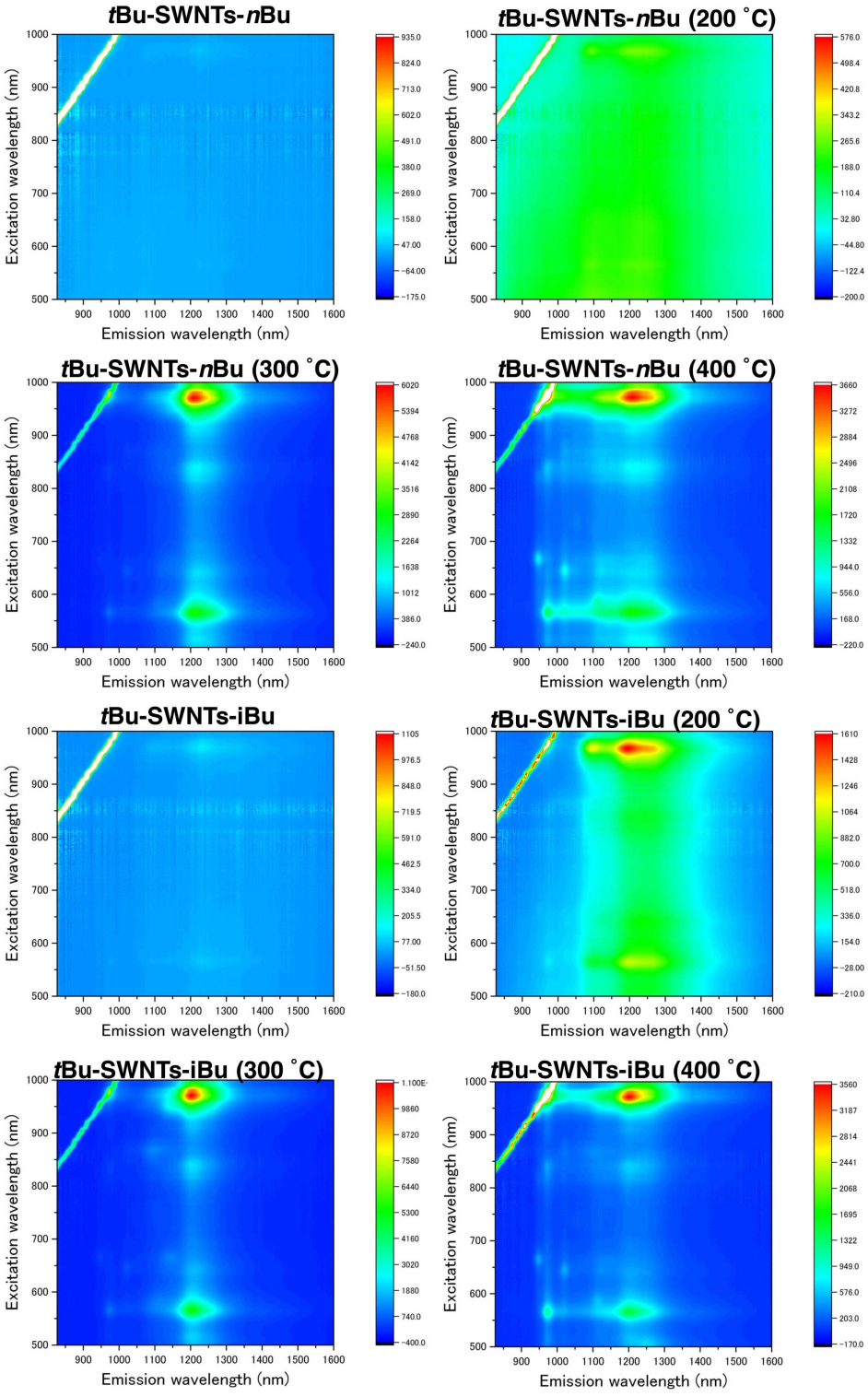

Figure S11. Contour plots of fluorescence intensity versus excitation and emission wavelength of SWNTs and *t*Bu-SWNTs-Bu before and after thermal treatment. The SWNTs were dispersed in D_2O containing SDBS.

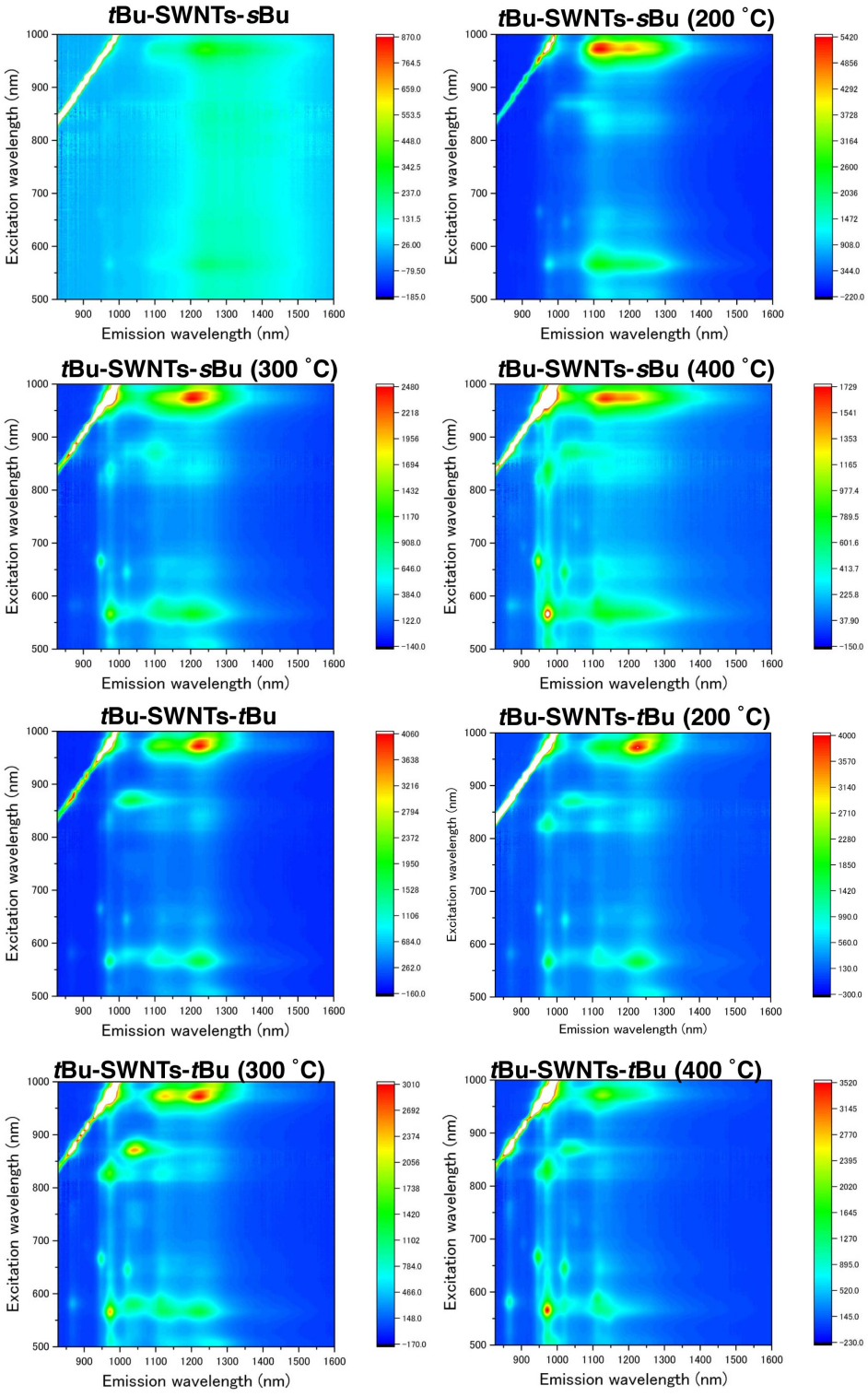

Figure S12. Contour plots of fluorescence intensity versus excitation and emission wavelength of SWNTs and *t*Bu-SWNTs-Bu before and after thermal treatment. The SWNTs were dispersed in D_2O containing SDBS.

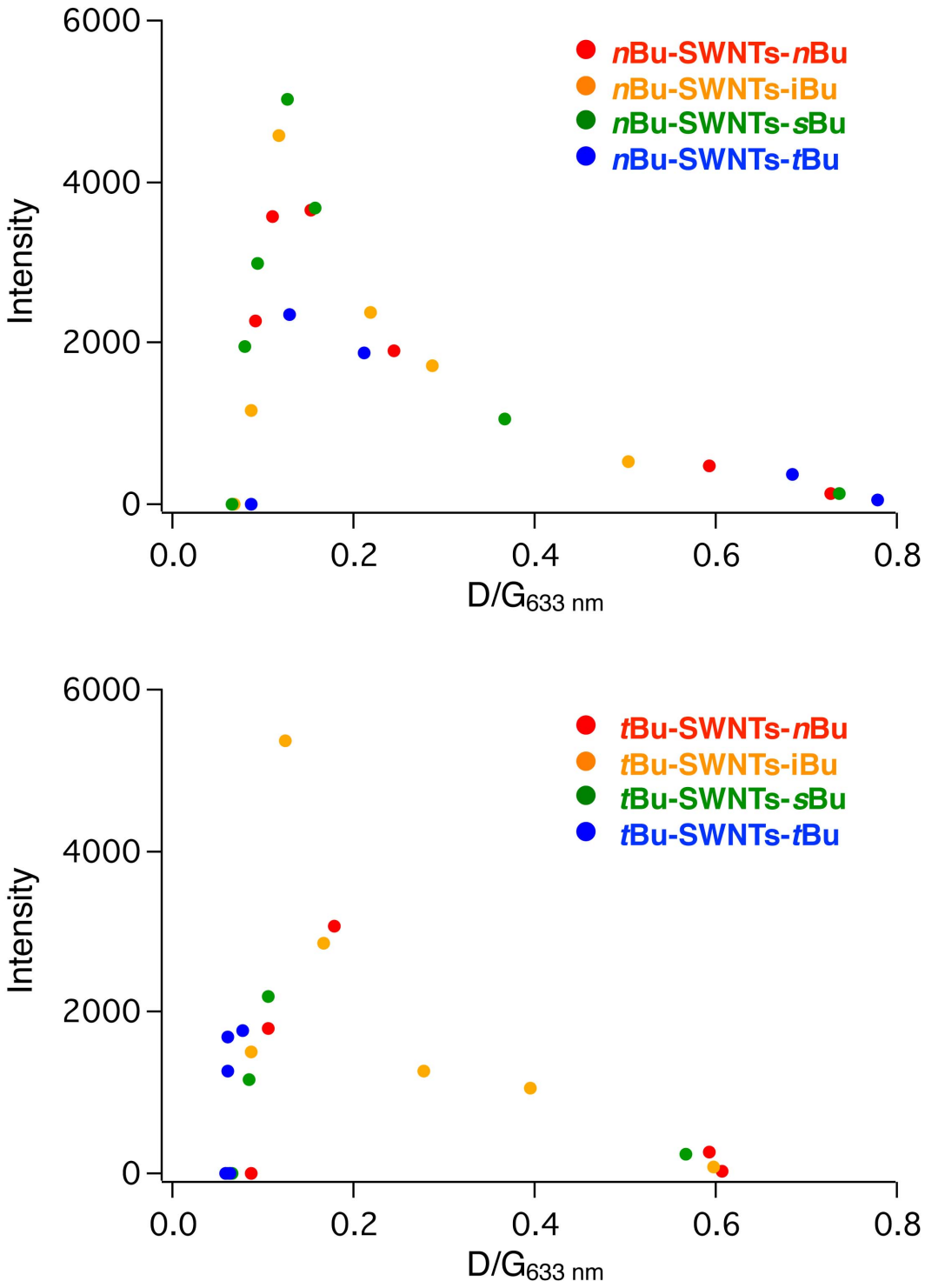

Figure S13. PL peak intensity of R-SWNTs-R and R-SWNTs-R(Δ) around 1.0 eV as a function of D/G_{633nm}.

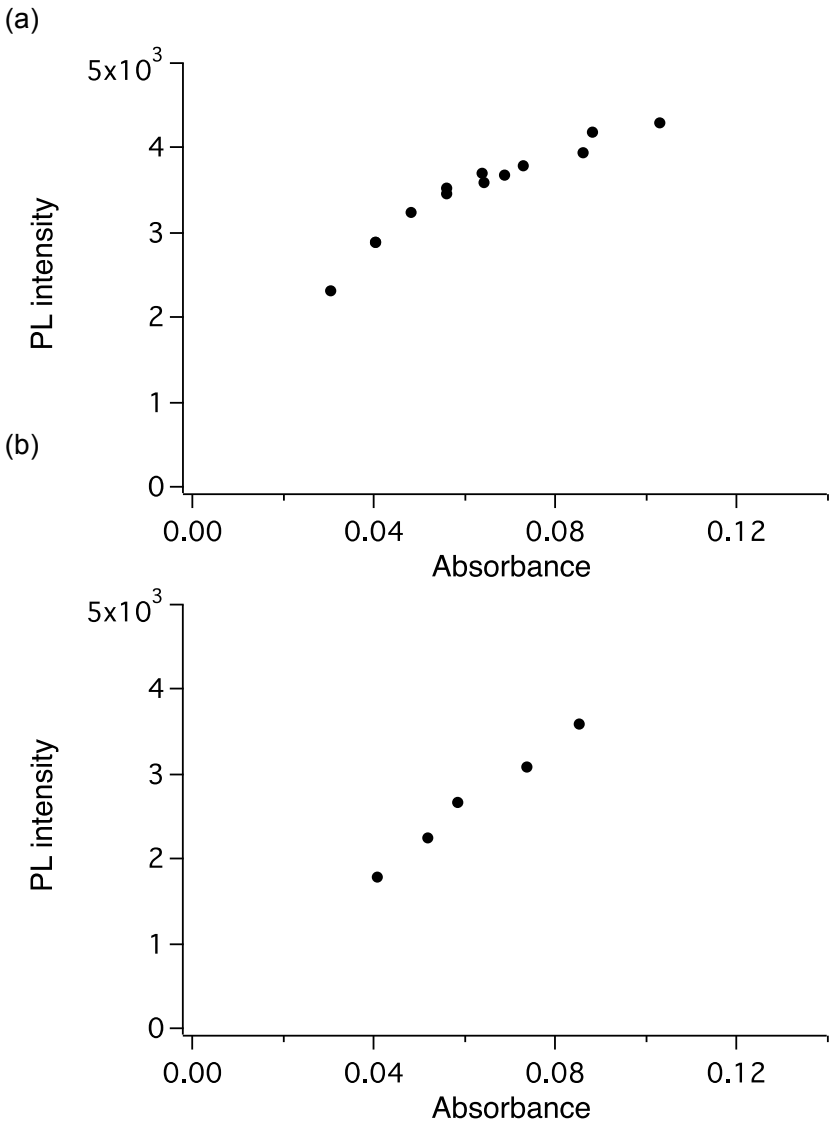

Figure S14. PL intensity of (a) SWNTs and (b) *n*Bu-SWNTs-*n*Bu (300 ˚C) as a function of the absorption intensity of local minimum around 775 nm.

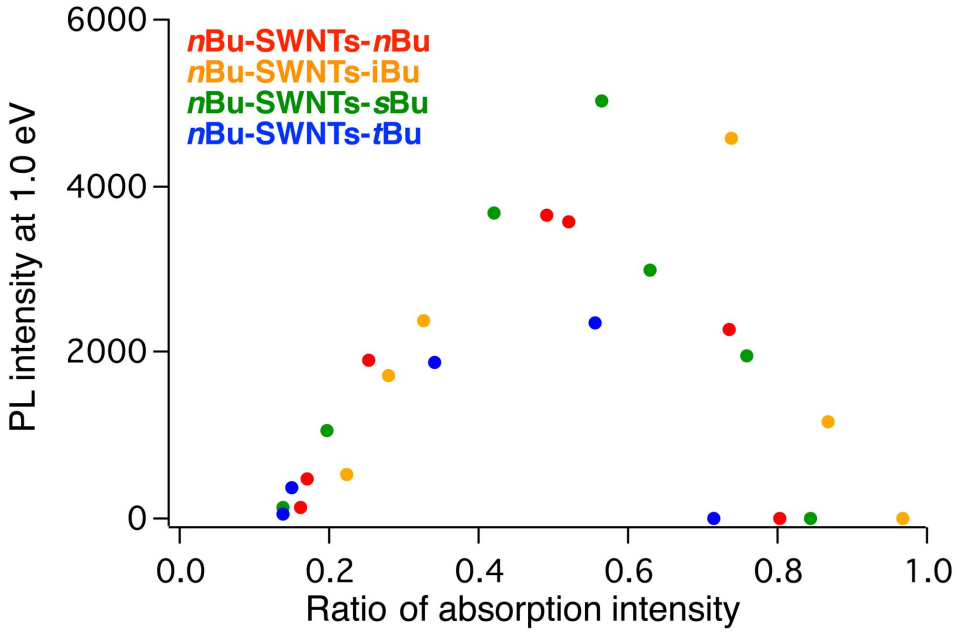

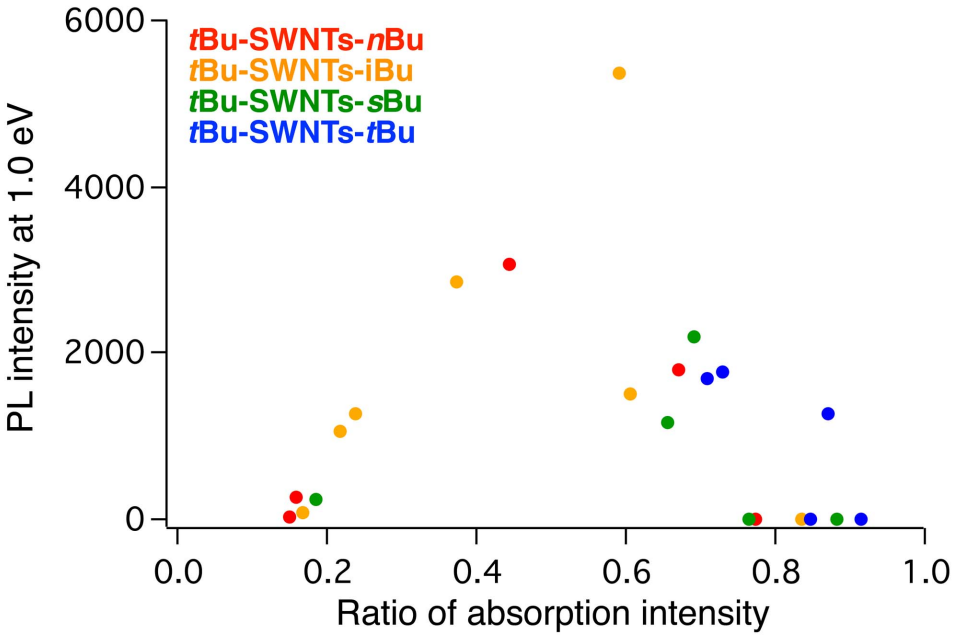

$$\text{Ratio of absorption intensity} = \frac{\text{Bu-SWNTs-Bu}_{970\text{nm}} / \text{Bu-SWNTs-Bu}_{767\text{nm}}}{\text{SWNTs}_{970\text{nm}} / \text{SWNTs}_{767\text{nm}}}$$

Figure S15. PL peak intensity of R-SWNTs-R and R-SWNTs-R(Δ) around 1.0 eV as a function of ratio of absorption intensity.

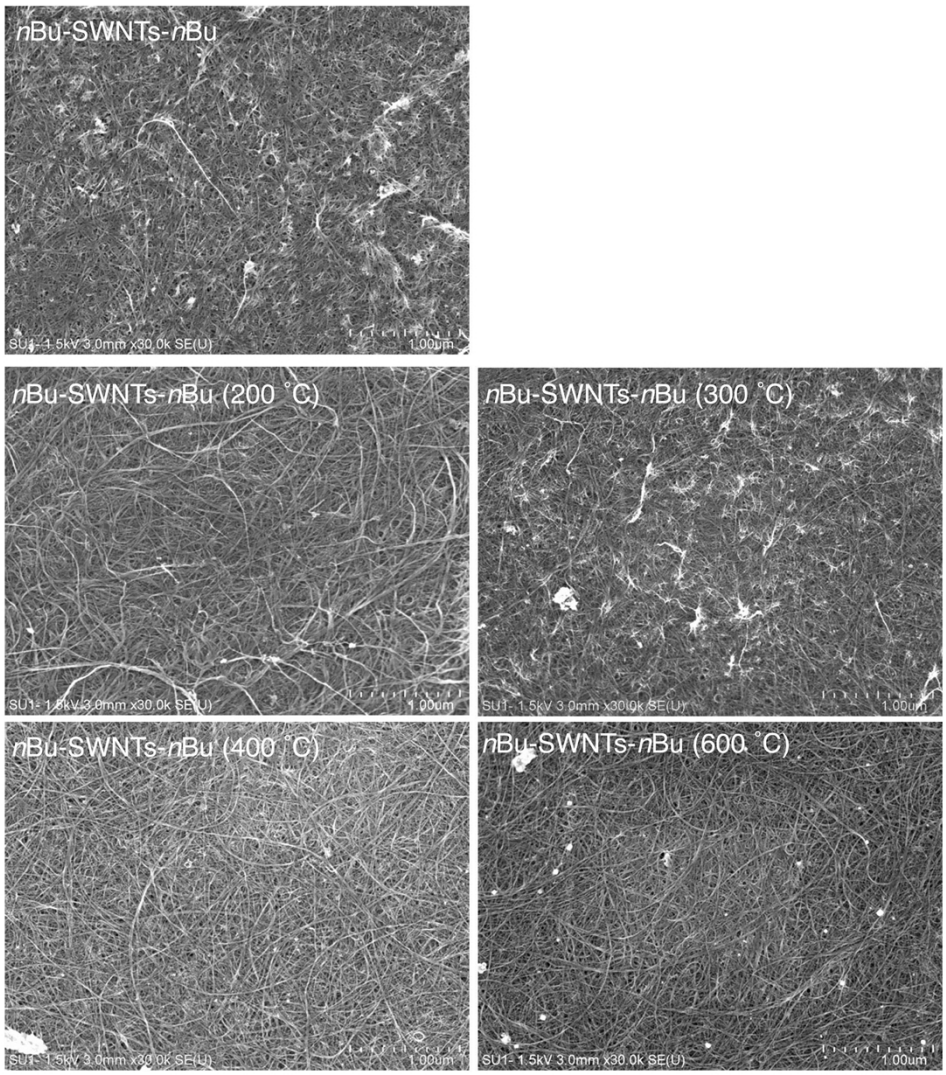

Figure S16. SEM images of SWNTs and *n*Bu-SWNTs-*n*Bu.

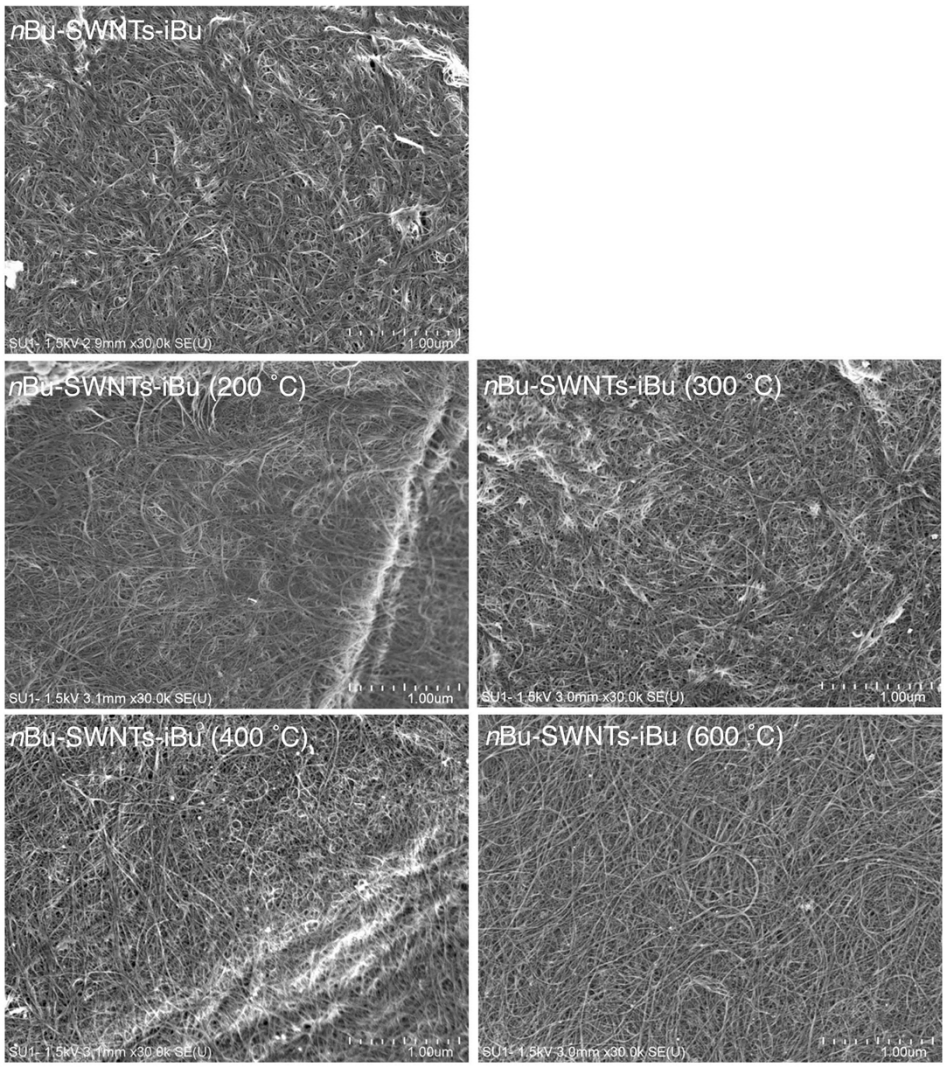

Figure S17. SEM images of SWNTs and *n*Bu-SWNTs-iBu.

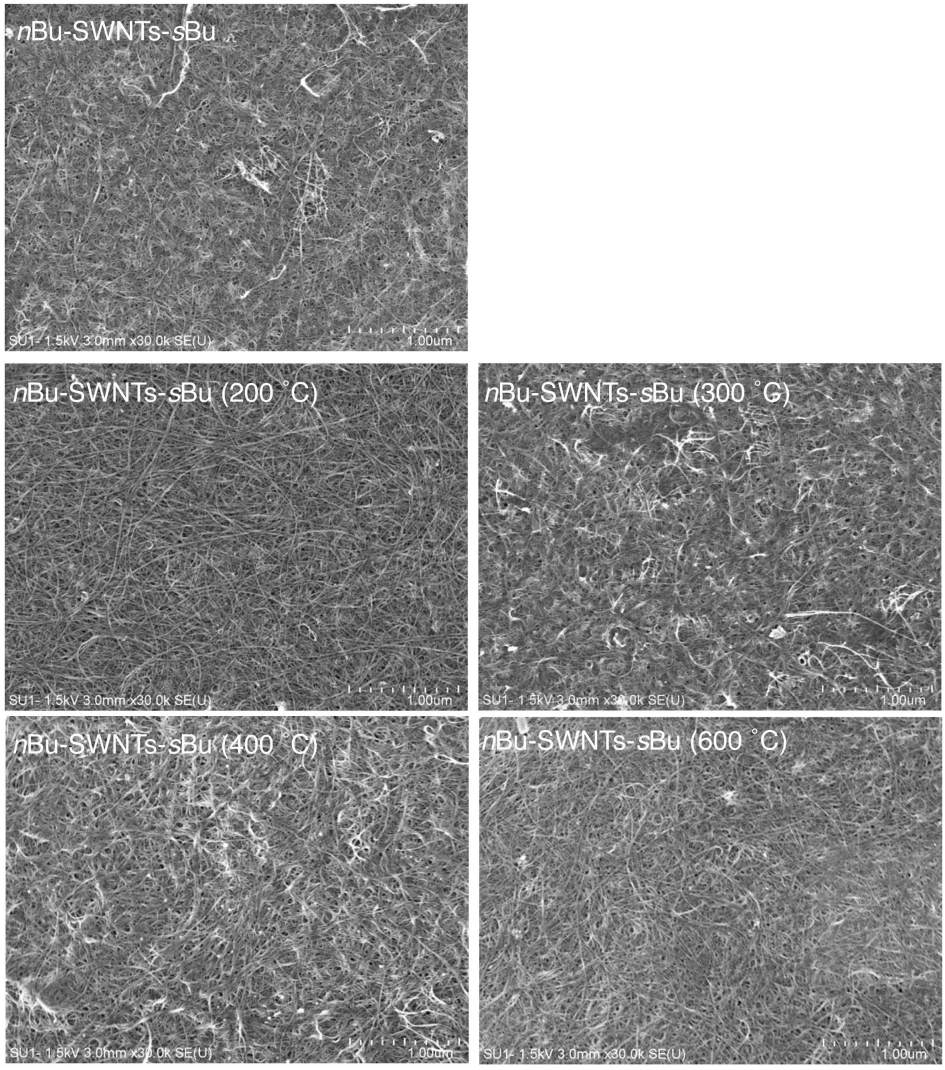

Figure S18. SEM images of SWNTs and *n*Bu-SWNTs-*s*Bu.

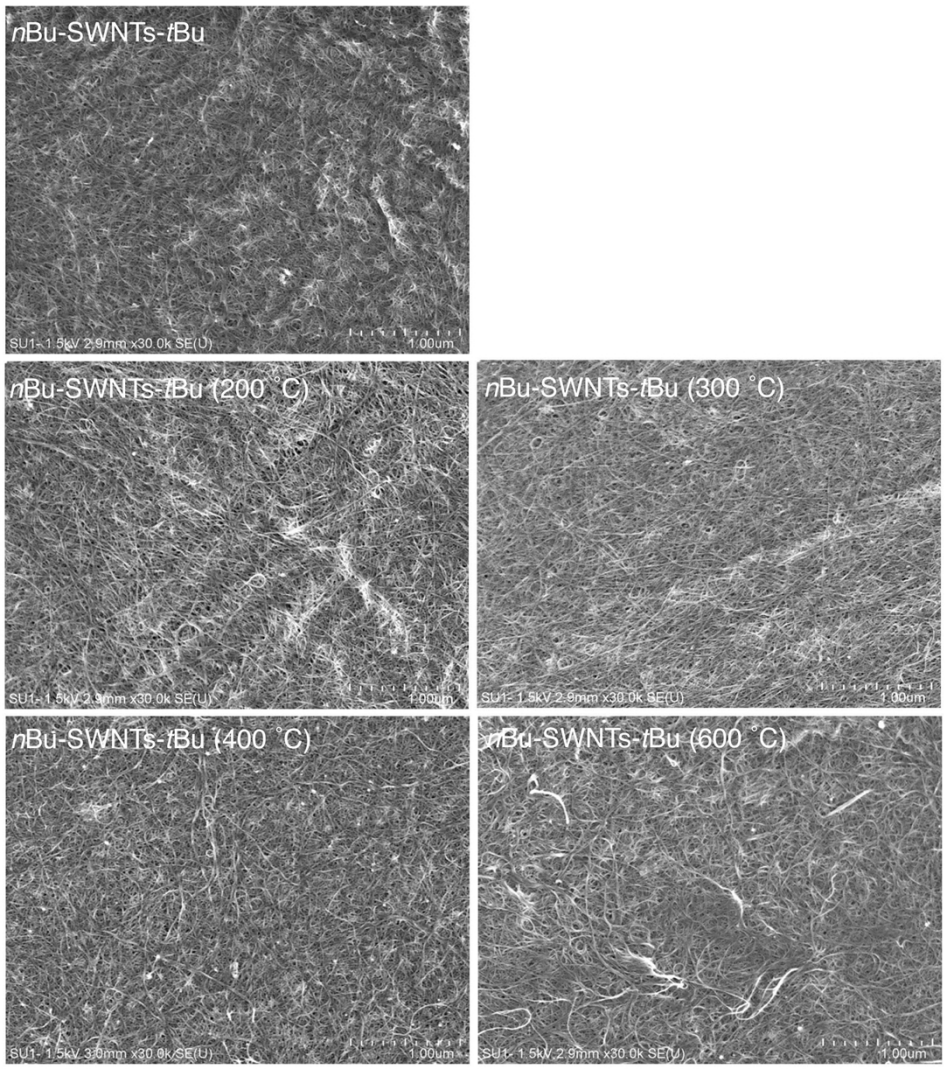

Figure S19. SEM images of SWNTs and *n*Bu-SWNTs-*t*Bu.

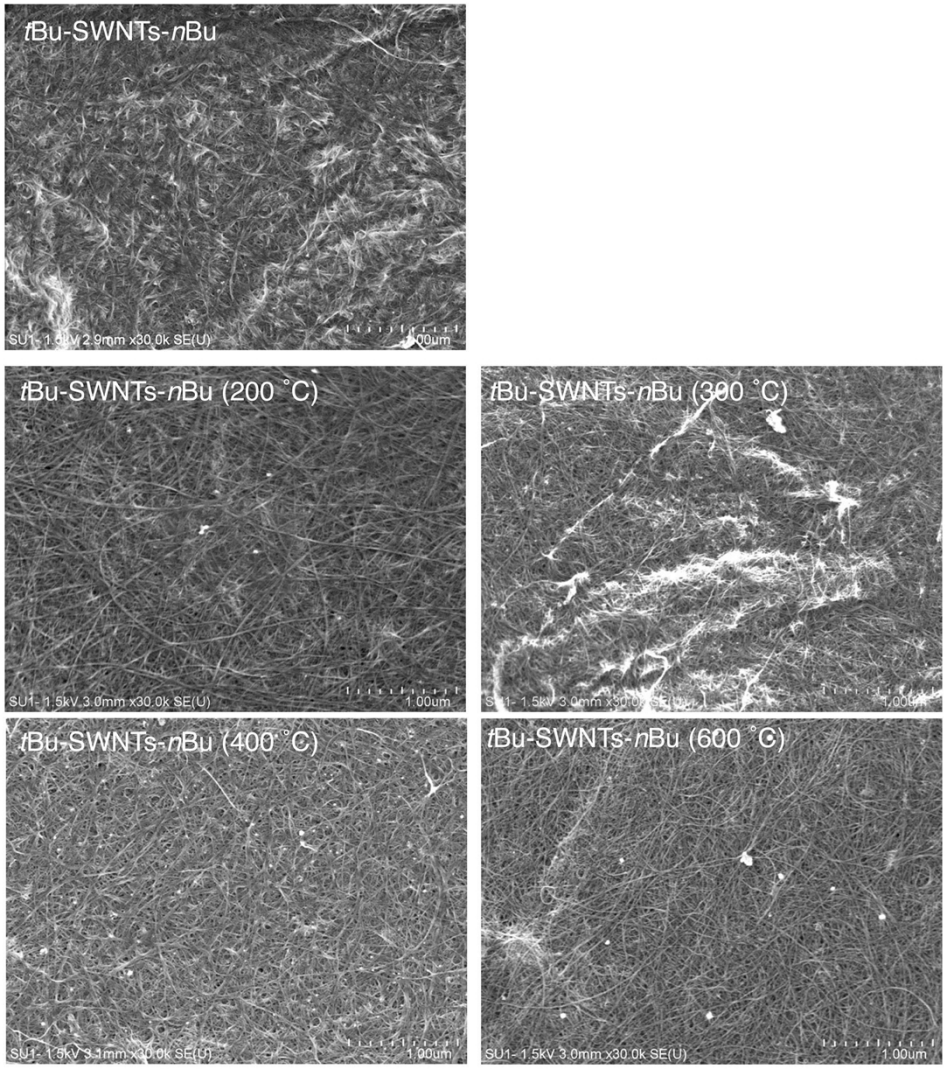

Figure S20. SEM images of SWNTs and *t*Bu-SWNTs-*n*Bu.

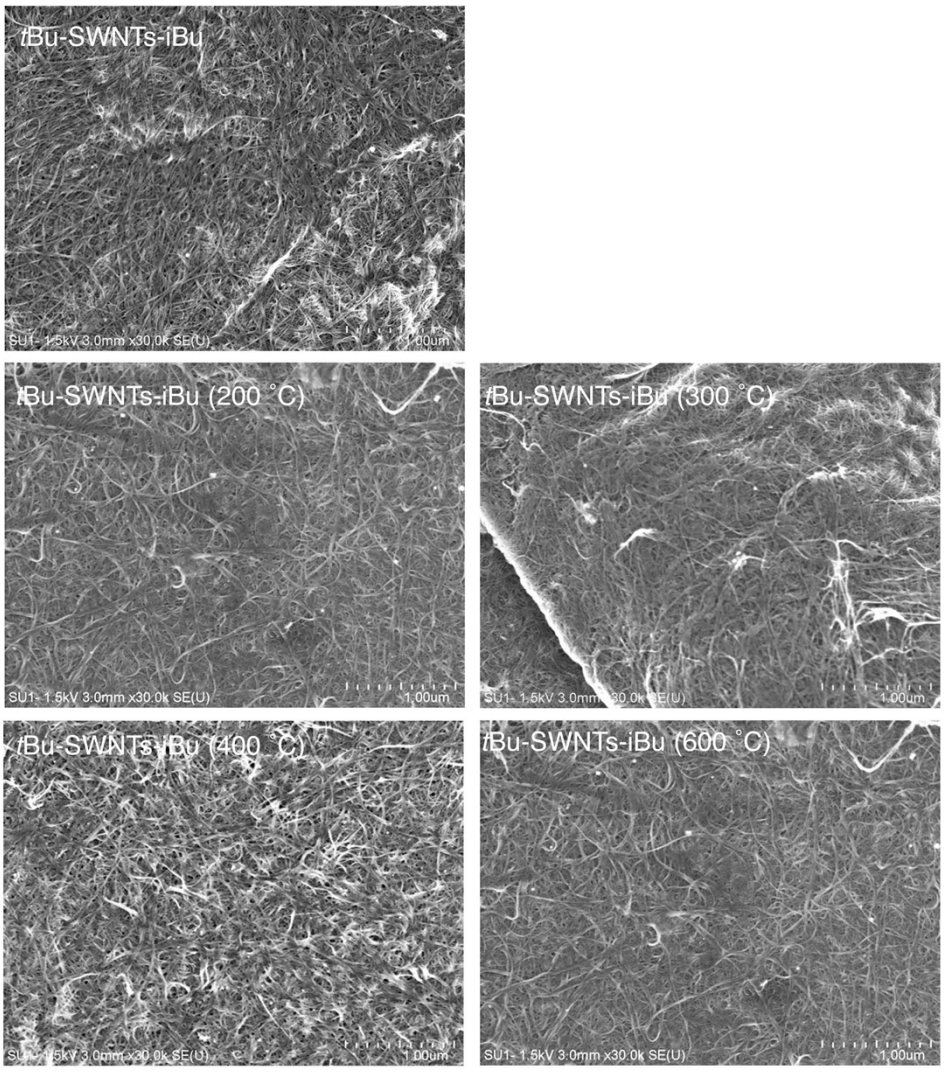

Figure S21. SEM images of SWNTs and *t*Bu-SWNTs-iBu.

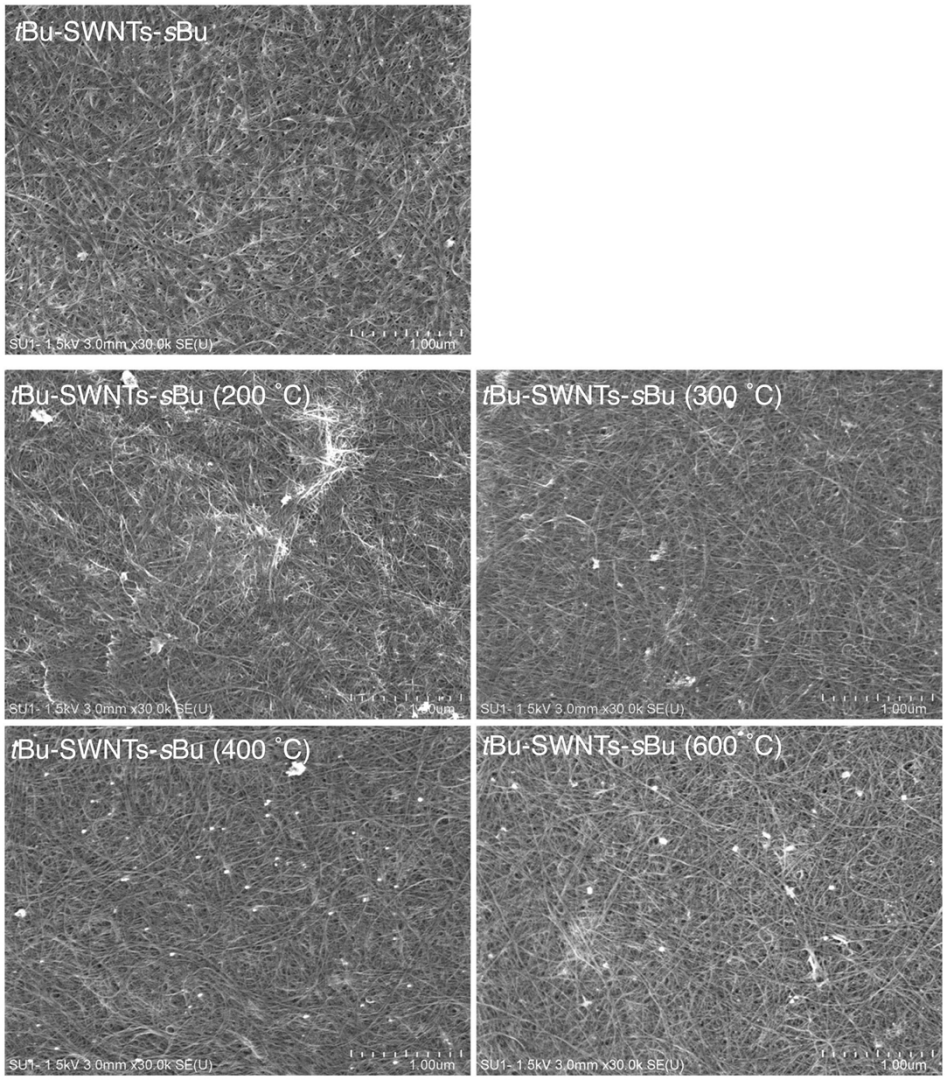

Figure S22. SEM images of SWNTs and *t*Bu-SWNTs-*s*Bu.

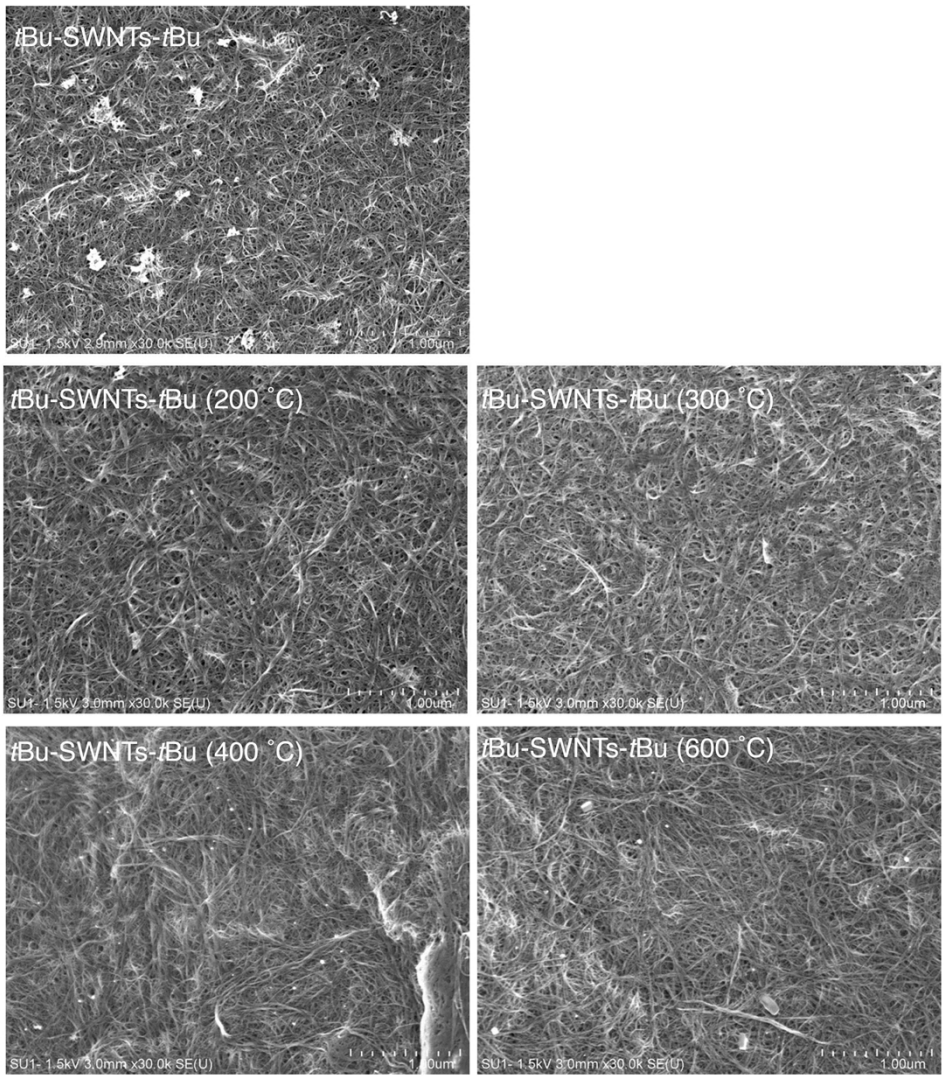

Figure S23. SEM images of SWNTs and *t*Bu-SWNTs-*t*Bu.

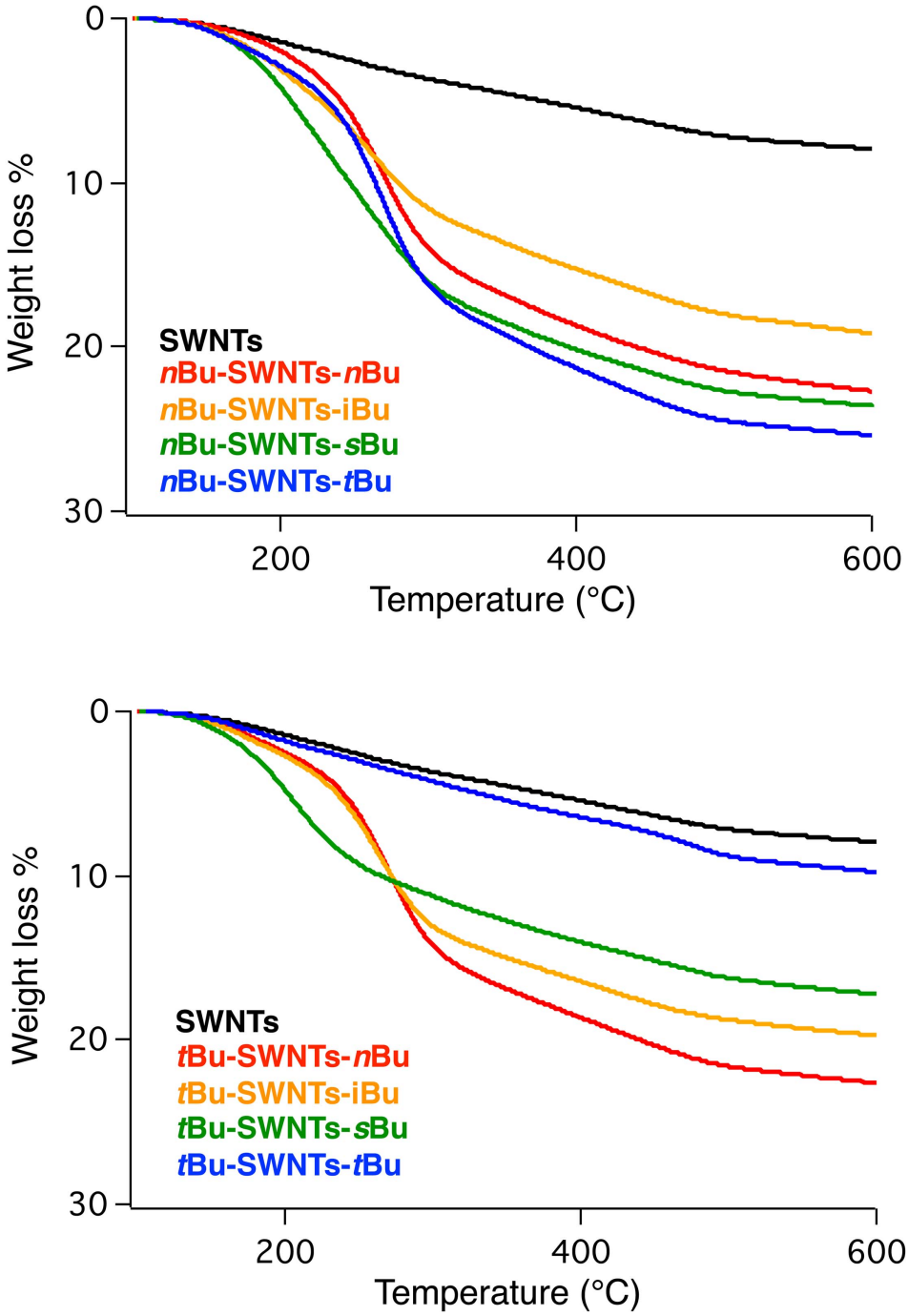

Figure S24. TG curves of SWNTs and Bu-SWNTs-Bu from 100 to 600 °C at a heating rate of 10 °C/min in N_2 atmosphere (50 ml/min).

Table S1. Absorbance around 775 nm and D/G of SWNTs and Bu-SWNTs-Bu.

SWNTs	$D/G_{514.5\ nm}$	$D/G_{633\ nm}$	Absorbance around 775 nm		Excitation wavelength (nm)	
			wavelength (nm)	intensity	E_{22}	E_{11}
SWNTs(before reaction)	0.07	0.04	779	0.084	566	
*n*Bu-SWNTs-*n*Bu	0.66	0.73	785	0.075	564	969
*n*Bu-SWNTs-*n*Bu (200 ˚C)	0.60	0.59	785	0.077	564	970
*n*Bu-SWNTs-*n*Bu (300 ˚C)	0.29	0.15	763	0.071	566	971
*n*Bu-SWNTs-*n*Bu (400 ˚C)	0.19	0.09	760	0.078	565	970
*n*Bu-SWNTs-*n*Bu (600 ˚C)	0.12	0.07	760	0.076	567	971
*n*Bu-SWNTs-iBu	0.53	0.50	774	0.066	568	969
*n*Bu-SWNTs-iBu (200 ˚C)	0.36	0.29	768	0.063	565	968
*n*Bu-SWNTs-iBu (300 ˚C)	0.16	0.09	773	0.077	566	971
*n*Bu-SWNTs-iBu (400 ˚C)	0.14	0.07	779	0.057	566	972
*n*Bu-SWNTs-iBu (600 ˚C)	0.09	0.06	779	0.062	566	971
*n*Bu-SWNTs-*s*Bu	0.68	0.74	785	0.083	565	968
*n*Bu-SWNTs-*s*Bu (200 ˚C)	0.44	0.37	785	0.080	566	669
*n*Bu-SWNTs-*s*Bu (300 ˚C)	0.24	0.13	768	0.077	565	971
*n*Bu-SWNTs-*s*Bu (400 ˚C)	0.16	0.08	764	0.079	565	971
*n*Bu-SWNTs-*s*Bu (600 ˚C)	0.11	0.07	776	0.079	566	971
*n*Bu-SWNTs-*t*Bu	0.68	0.78	785	0.068	562	971
*n*Bu-SWNTs-*t*Bu (200 ˚C)	0.65	0.69	785	0.078	566	970
*n*Bu-SWNTs-*t*Bu (300 ˚C)	0.36	0.21	760	0.076	565	970
*n*Bu-SWNTs-*t*Bu (400 ˚C)	0.24	0.13	764	0.087	566	971
*n*Bu-SWNTs-*t*Bu (600 ˚C)	0.14	0.09	765	0.070	566	969
*t*Bu-SWNTs-*n*Bu	0.63	0.61	785	0.051	565	966
*t*Bu-SWNTs-*n*Bu (200 ˚C)	0.58	0.59	785	0.063	565	970
*t*Bu-SWNTs-*n*Bu (300 ˚C)	0.31	0.18	764	0.068	566	971
*t*Bu-SWNTs-*n*Bu (400 ˚C)	0.20	0.11	764	0.068	566	971
*t*Bu-SWNTs-*n*Bu (600 ˚C)	0.11	0.09	764	0.062	566	970
*t*Bu-SWNTs-iBu	0.59	0.60	785	0.063	566	969
*t*Bu-SWNTs-iBu (200 ˚C)	0.44	0.40	776	0.072	566	968
*t*Bu-SWNTs-iBu (300 ˚C)	0.19	0.12	765	0.081	566	971
*t*Bu-SWNTs-iBu (400 ˚C)	0.15	0.09	778	0.066	566	971
*t*Bu-SWNTs-iBu (600 ˚C)	0.11	0.07	778	0.069	566	971
*t*Bu-SWNTs-*s*Bu	0.58	0.57	785	0.077	565	971
*t*Bu-SWNTs-*s*Bu (200 ˚C)	0.16	0.11	765	0.079	566	971
*t*Bu-SWNTs-*s*Bu (300 ˚C)	0.15	0.08	767	0.081	566	972
*t*Bu-SWNTs-*s*Bu (400 ˚C)	0.12	0.07	777	0.075	566	972
*t*Bu-SWNTs-*s*Bu (600 ˚C)	0.09	0.06	777	0.081	566	972
*t*Bu-SWNTs-*t*Bu	0.11	0.08	778	0.076	566	972
*t*Bu-SWNTs-*t*Bu (200 ˚C)	0.09	0.06	779	0.071	566	972
*t*Bu-SWNTs-*t*Bu (300 ˚C)	0.10	0.06	780	0.069	566	971
*t*Bu-SWNTs-*t*Bu (400 ˚C)	0.09	0.06	778	0.091	566	971
*t*Bu-SWNTs-*t*Bu (600 ˚C)	0.10	0.06	781	0.060	566	971

Table S2. PL peak area and relative PL peak area toward SWNTs (Ex: E_{22} 0.775 – 1.5 eV; E_{11} 0.775 – 1.2 eV).

SWNTs	Absorbance around 775 nm		Excitation	Emission peak area[1]								Sum of peak	Peak area ratio
	wavelength (nm)	intensity	wavelength (nm)	1.43 eV	1.27 eV	1.22 eV	1.17 eV	1.10 eV	1.03 eV	0.99 eV	0.86 eV	area[2]	toward SWNTs
SWNTs	779	0.084	E_{22} 565	20.4	180	28.7		180				409	
*n*Bu-SWNTs-*n*Bu (300 ˚C)	763	0.071	E_{22} 566		18.8	11.7		27.2	214	242	10.0	524	1.3
			E_{11} 971					46.8	483	386	17.9	934	2.3
*n*Bu-SWNTs-iBu (300 ˚C)	773	0.077	E_{22} 566		30.3	23.5		40.3	319	276	14.2	703	1.7
			E_{11} 971					155	773	299	19.5	1247	3.0
*n*Bu-SWNTs-*s*Bu (300 ˚C)	768	0.077	E_{22} 565		30.3	23.5		40.3	319	276	14.2	703	1.7
			E_{11} 971					55.4	657	482	24.3	1218	3.0
*n*Bu-SWNTs-*t*Bu (400 ˚C)	764	0.087	E_{22} 567		33.0	52.6	59.7	21.6	29.2	24.6	0.53	221	0.5
			E_{11} 971				125	213	293	296		927	2.3
*t*Bu-SWNTs-*n*Bu (300 ˚C)	764	0.068	E_{22} 566		15.5	9.07		16.5	170	221	9.60	441	1.1
			E_{11} 971					23.6	368	358	17.2	768	1.9
*t*Bu-SWNTs-iBu (300 ˚C)	765	0.081	E_{22} 565		36.5	13.1		60.0	355	226	15.5	706	1.7
			E_{11} 971					56.3	788	368	30.0	1243	3.0
*t*Bu-SWNTs-*s*Bu (200 ˚C)	765	0.078	E_{22} 566		46.0	18.0		258	191	143		655	1.6
			E_{11} 971					423	397	326		1146	2.8
*t*Bu-SWNTs-*t*Bu	778	0.076	E_{22} 566	1.3	63.5	41.0		136	149	24.9	4.10	419	1.0
			E_{11} 971					180	404	206	13.3	803	2.0

1 Lorentzian curve fitting data. 2 Sum of curve fitting data.